UDC 531.788.6:621.3.083.92

V.V. BUNIATYAN, V.K. BEGOYAN, H.H. HOVNIKYAN, A.A. DAVTYAN

THE METAL - $Ba_xSr_{1-x}TiO_3$- METAL THIN FILM STRUCTURE C-V, G-V CHARACTERISTICS

A new model of *C–V* (*g–V)* dependencies of thin film metal- $Ba_xSr_{1-x}TiO_3$-metal *(m-f-m*) structure is considered. Analytical expressions are derived for C–V, g–V and loss tangent dependencies. Theoretical results are compared with the experimental data, and good agreement has been obtained.

Keywords: ferroelectric, oxygen vacancy, C-V dependencies, Pool-Frenkel emission.

1. INTRODUCTION

Integrating the perovskite-type transition metal oxides with the silicon–based semiconductor technology would introduce the possibility to develop multifunctional microelectronic devices such as field–effect transistors [1], nonvolatile ferroelectric random access memory (FRAM)[2], surface acoustic wave resonators and tunable varactors [3], chemical and biosensors, transducers (including ultrasonic, infrared and imaginary applications) [4-8], micromechanical systems (MEMS) [3-5], etc.

Derived mainly by this application, the *C-V (C-T), g-V(g-T)* dependencies, loss mechanisms, as well as the experimental hysteresis effects in thin BST film - based devices have been subjects for extensive studies [1-4, 9]. The main task of this work is the analysis and interpretation of the experimental results including the impact of defects on the performances of the devices. It is shown that the shape of the *C-V (C-T), g-V (g-T)* curves strongly depend on the conduction mechanisms (SCL, Schottky, Tunnel, Fowler-Nordheim, Pool-Frenkel, etc.), on the presence of oxygen vacancies (as the inevitable defects in ferroelectric materials), nature and density of the interface states, traps, etc [1- 4]. To the best of the author's knowledge, there are relatively few studies in which the electro-physical processes, such as the nonlinearity of permittivity, the trapping/detrapping of charge carriers by oxygen vacancies are involved for modeling the C-V, *g -V* dependencies and hysteresis. In this work ,we offer new approaches to derive analytical expressions for the above mentioned C-V, *g-V* dependencies, which allow, in turn, for easy modeling of these characteristics and explicit interpretation of all experimental results obtained by different authors.

2. THE MODEL

The model is based on the assumptions that: a) the dielectric permittivity of ferroelectric materials is the nonlinear dependence of the applied electric field $\varepsilon(E,r) = \varepsilon(0)(1 + AE^2)^{-1}$, where $A = 3\beta(\varepsilon_0\varepsilon(0))^3$, and $\varepsilon(0)$ is the permittivity at a zero bias, ε_0 is the vacuum dielectric constant. For example, for $SrTiO_3$, β =8x10^{9}V·m^5/C^3, $\mathcal{E}$ (0)=106, and A=0.45·10^{-15} (m/V)^2, b) in the interfacial regions of metal-ferroelectric contacts, the oxygen vacancy concentration is high which "endowed" the ferroelectric to n-type semiconductor properties[1,3,9], c) these oxygen vacancies create electron trap levels in the band gap of the ferroelectric, d) with increasing the applied electric field, the traps release electrons via Poole-Frenkel mechanism and become charged [10]. The three layer model is considered in Fig.1. It is assumed that the concentration of the oxygen vacancies is large at the interfacial with the metal (Pt) contact region, and that some of these vacancies trap electrons and create space – charge regions. For simplicity, both metal/ferroelectric contacts are assumed to be identical. The density of the oxygen vacancies in the middle part of the ferroelectric film (core) is assumed to be relatively low. The work function (~5.6eV) of Pt is greater than that of the ferroelectric film (~3.2 eV) which means that the currents will be emission–limited. In equilibrium and at very low temperatures all of the trapped electrons (holes) would be in traps: at high temperatures and in the presence of an applied field, some of these electrons (holes) will be exited into shallow traps or conduction levels, either thermally or due to the action of the field [1,3,9].

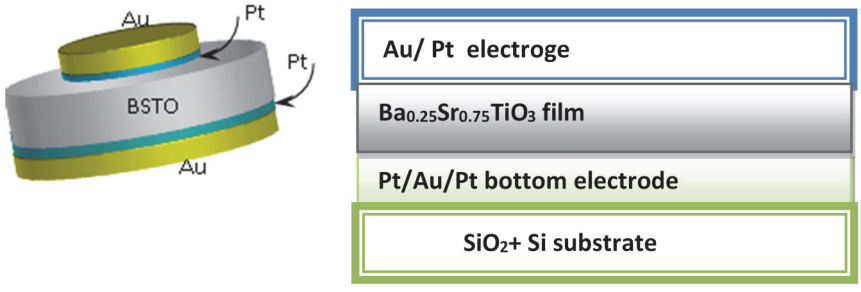

a b

Fig.1.The structure of a thin film Pt/BSTO/Pt capacitor (a) and secuentance of layers (b)

The model based on the assumptions that: a) the dielectric permittivity of ferroelectric materials is a nonlinear dependance of the applied electric field $\varepsilon(E,r) = \varepsilon(0)(1 + AE^2)^{-1}$, where $A=3\beta(\varepsilon_0\varepsilon(0))^3$, and $\varepsilon(0)$ is the permittivity at a

zero bias, ε_0 is the vacuum dielectric constant. For example, for $SrTiO_3$, β=8x10^{9}V·m^5/C^3, $\varepsilon(0)$=106,and A=0.45·10^{-15}(m/V)^2,b) in interfacial regions of metal-ferroelectric contacts the oxygen vacancy concentration is high which "endowed" the ferroelectric to the n –type semiconductorproperties, c) these oxygen vacancies create electron trap levels in the band gap of the ferroelectric, d) with increasing the applied electric field, the traps release electrons via Poole-Frenkel mechanism and become charged, f) We assume that $\tau_{\mathrm{t}} \ll \omega^{-1}$, i.e. the transit time of electrons, τ_{t}, through the film is small in comparison of the measure signal frequency ω^{-1}.

Based on the assumptions' a) - f), solving the current density equation

$$j_i = S\left\{i\omega\frac{\varepsilon_r}{\beta}\cdot E_{1m} + q\cdot\mu\cdot E_0\cdot n_{1m} + q\mu E_{1m}\cdot n_0\right\},$$

where S is the cross section area of the film, ω is the applied alternating signal's frequency, $\varepsilon_r = \varepsilon_0\varepsilon(0)$, q is the elementary charge, μ is the mobility of electrons, E_0 is the Dc electric field, E_{1m} is the alternating component of the electric field, n_0 is the free electron concentration (including SCL, Schottky injectionand Pool-Frenkel emission), for the capacitance, conductance and loss tangent, we have obtained:

$$C_0 = \frac{S\cdot\varepsilon_g}{\beta\cdot l} = \frac{S\cdot\varepsilon_r\cdot\omega(0)\cdot l^2}{(l^2+A\cdot U_0^2)\cdot l} = \frac{S\cdot\varepsilon_r\cdot l}{l^2+A\cdot U_0^2},\ C_t = \frac{2S\cdot\varepsilon_r\cdot\mu\cdot b_1\cdot U_0(b_1^2+\omega^2)(l^2-A\cdot U_0^2)\cdot S_n^2\cdot\gamma\cdot N_t}{l\cdot(l^2+A\cdot U_0^2)^2(b_2^2+b_3^2)},$$

$$g_t = \frac{2S\cdot\varepsilon_r\cdot\mu(l^2-A\cdot U_0^2)b_2\cdot b_1(b_1^2+\omega^2)\cdot U_0}{l\cdot(l^2+A\cdot U_0^2)^2(b_2^2+b_3^2)}, b_3 = \omega\cdot S_n^2\cdot\gamma\cdot N_t, b_1 = S_n(\gamma+n_0),$$

$$g_0 = \frac{S\cdot q\cdot\mu\cdot n_0}{l},\ \gamma(E_t) = \frac{N_C}{g}exp(\frac{E_t-F}{kT}),\ b_2 = b_1[(b_1{}^2+\omega^2)+S_n{}^2\gamma N_t],$$

$$tg\delta = \frac{10^{-6}(g_0+g_t)}{6.28\cdot f(C_0+C_t)}, \quad (1)$$

where C_0 and g_0 are the geometrical capacitance and DC conductance of the *m-f-m* structure, recpectively, l is the length of the ferroelectric film, U_0 is the applied DC voltage, , C_t and g_t are the so called "trapping" dynamic capacitance and conductivity, respectively, n_i is the concentration of injected electrons, n_{pF} is the concentration of electrons realized via Pool-Frenkel emission, F is the imref, E_C is the conductance band bottom energy, k is the Bolltsmann's constant, T is the

absolute temperature, N_c is the density of the states in the conduction band, N_t is the concentration of the oxygen vacancies near the metal contact, E_t is the energy of the trap level in respect of the edge of the ferroelectric conductance band, $\gamma(E_t)$ is the Shockley–Read start-factor, g is the degeneracy factor and g=2[11Sze], $S_n = < V_{th}\ \sigma >$ is the trap capture rate, V_{th} is the thermal velocity of electrons, σ is the capture cross section. As it follows from the expressions of C_t and g_t, both depend on the applied alternating signal's frequency ω, as well as strongly depend on the concentration of oxygen vacancies and its energy distribution via the parameters of b_1,b_2, b_3.

Numerical calculations have been carried out according to Eq.1 for the follow parameters of ferroelectric BST films and output signal parameters**:

$$\mathrm{N_t} = (10^{16} \dots 10^{19})\mathrm{cm^{-3}}, l = (100 \dots 600)\mathrm{nm}, \mathrm{f} = (10^{6} \dots 10^{11})\mathrm{Hz}, \mathrm{n_0} = 10^{10} \dots 10^{13}\mathrm{cm^{-3}}, \mathrm{S} = 7 \cdot 10^{-6}\mathrm{cm^2}, \varepsilon_g == 8.85 \cdot 10^{-14} \cdot \varepsilon(0)_{(\mathrm{BST})}, \mathrm{N_c} \approx 10\mathrm{cm^{-3}},$$

$$\mu = (0.01 \dots 30)\frac{\mathrm{cm^2}}{\mathrm{V \cdot s}}, \mathrm{U_0} = (-20 \dots + 20)\mathrm{V}, \sigma = (10^{-14} \dots 10^{-16})\mathrm{cm^2}, \mathrm{V_{th}} \approx\approx 10^{7}\mathrm{cm/s}, \Delta\mathrm{E_t} = (0.06 \dots 0.4)\mathrm{eV}, \varepsilon(0)=106_{(\mathrm{BST})}.$$

The results of theoretical calculations and experimental investigations of *m-BST-m* structures are presented in Fig.2. For comparison of theoretical and experimental data, the values of these parameters were taken from the experimentally investigated real structures carried out in [3,4,9], as well as by other authors [12]. In Fig.2 a,b the experimental research results of the thin test varactors are presented which are fabricated by RF magnetic sputtering, using a $Ba_{0.5}Sr_{0.5}TiO_3$ target, and tested in Chalmers Technological University (Sweden) [3,4]. The films are 290...560 nm thick. In Fig.2 c, d, e., the theoretically calculated C-U_0 ($C=C_0+C_t$), $tg\delta - f$, (g_0+g_t)-U_0, dependencies according to (1) for the above mentioned parameters of the BST films are presented.

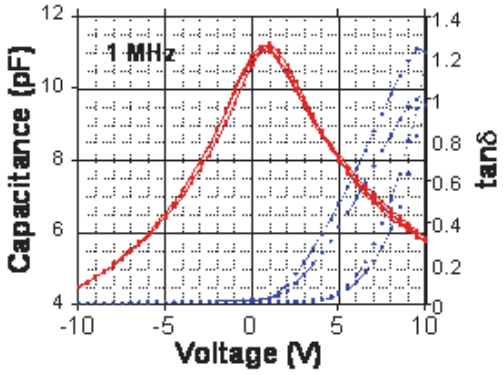
1 MHz
Capacitance (pF)
tanδ
Voltage (V)
12
10
8
6
4
1.4
1.2
1
0.8
0.6
0.4
0.2
0
-10
-5
0
5
10

a

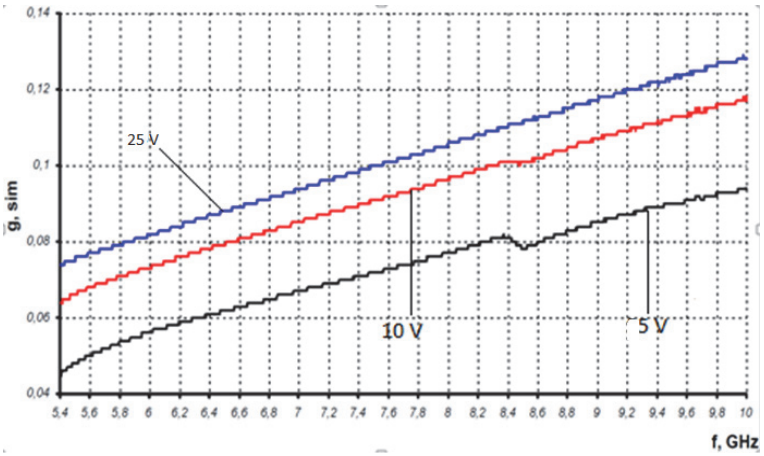
g, sim
f, GHz
25 V
10 V
5 V
0,14
0,12
0,1
0,08
0,06
0,04
5,4 5,6 5,8 6 6,2 6,4 6,6 6,8 7 7,2 7,4 7,6 7,8 8 8,2 8,4 8,6 8,8 9 9,2 9,4 9,6 9,8 10

b

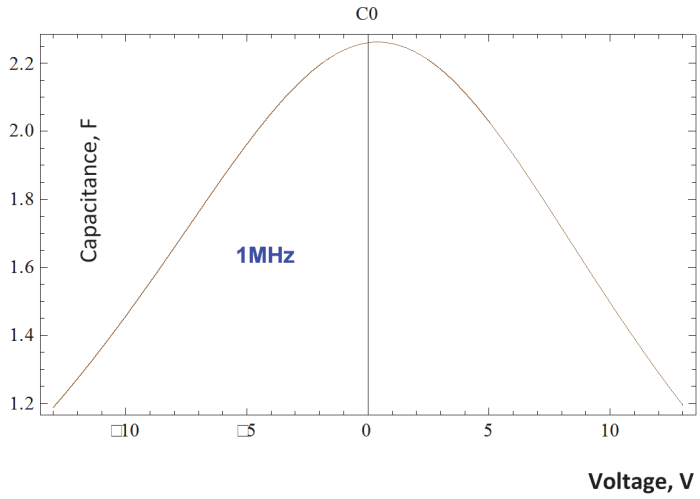
C0
Capacitance, F
1MHz
Voltage, V
2.2
2.0
1.8
1.6
1.4
1.2
□10
□5
0
5
10

c

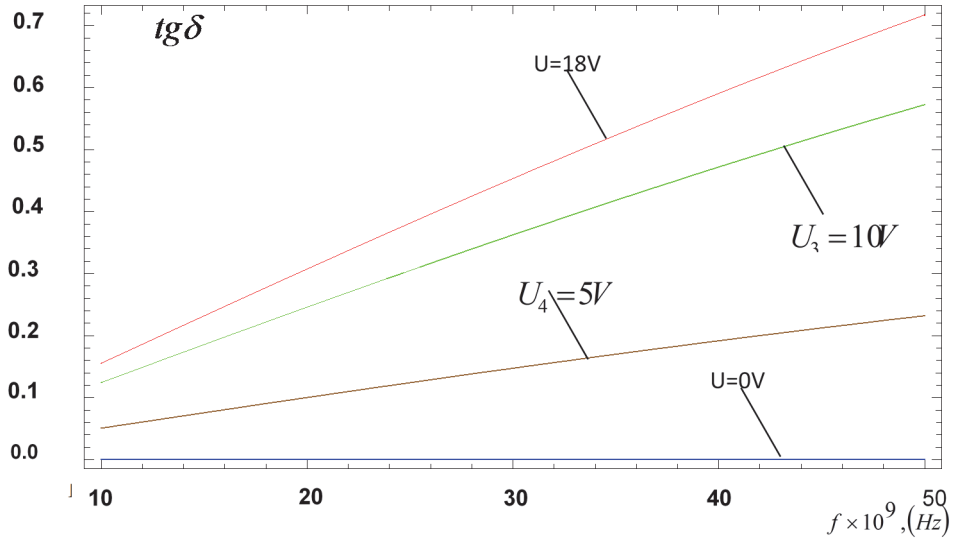

d

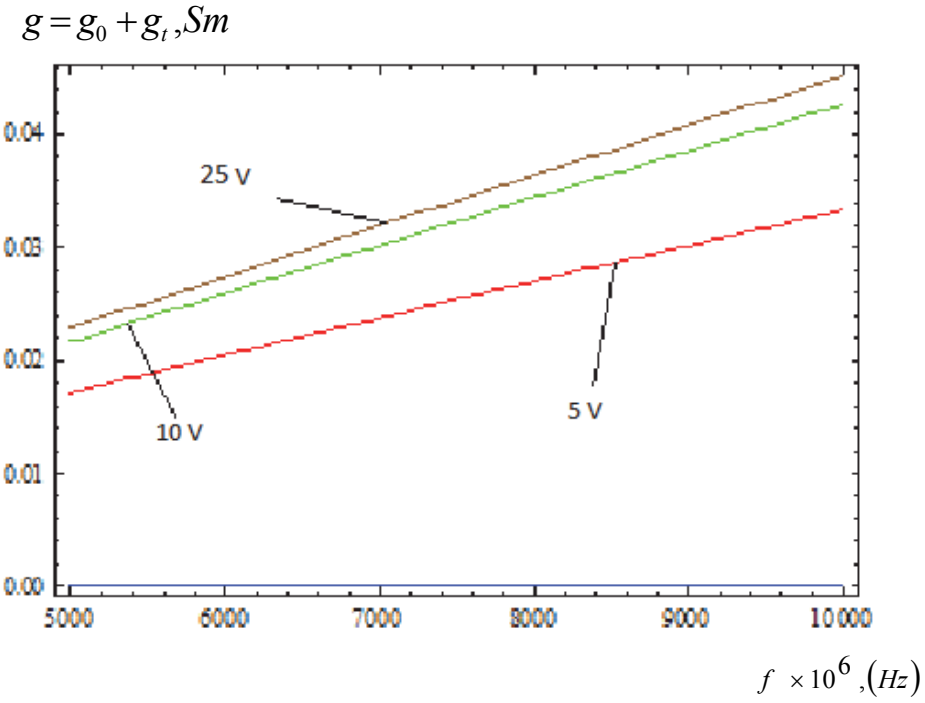

e

Fig. 2. The results of theoretical calculations and experimental investigations of m-BST-m structures

In Fig. 2, the experimental dependence of *C-U* and $tg\delta$ of the test varactor $Ba_{0.25}Sr_{0.75}$ TiO_3 on the applied voltage at the frequency 1.0 MHz (a), the experimental dependence of conductivity on frequency *f* for different values of the applied voltage (b) with the parameters: the area *S*=7x10^{-6}cm^2, l =290 nm [2,4-6], and theoretical (calculated) dependences of *C-U*$_0$ (c), $tg\delta - f$ (d), g-f (e), for different values of the applied voltages according to (1) with the parameters: trap concentration, $N_t = 10^{19} cm^{-3}$, E_t=0.26eV, μ=30cm^2/Vs, *f* =1.0MHz, σ=10^{-14} cm^2, area *S*=7x10^{-6}cm^2, l =290nm, n_0=10^{11}cm^{-3} .

3.CONCLUSIONS

The comparison of experimental and calculated results presented in Fig.2 shows that the theory and experiments are usually in good qualitatively agreement with each other. As it follows from expression (1), the "trapped" capacitance, C_t is forward and the "trapping" conductance, g_t is reversely proportional to the oxygen vacancy-conditioned trap concentration N_t, and in a complex form depends on the parameter $\gamma(E_t)$, that is the energy depth of trap levels E_t. The C_t and g_t depend on the capture cross section of traps, $S_n = \sigma \cdot V_{th}$, the signal frequency, ω, as well as depend on geometrical and material parameters of the ferroelectric thin films, such as: coefficient A, length, l, cross section area, S , dielectric permittivity, $\varepsilon(E,r)$ and applied signal parameters, U_0. The geometrical capacitance of structure C_0 will decrease with the increase of the applied field U_0, and the constant component of the geometrical conductance g_0 is forward proportional to the free concentration of electrons and its mobility. It follows from expressions (1), that the smaller the value of E_t, the higher of the free electron concentration and conductance are, all other conditions being equal. Moreover, under these conditions, the "trapped" capacitance will decrease with the increase in E_t, because of the decrease in the trapped electron concentration. Thus we can conclude that for design, mathematical modeling, characterization and theoretical calculations of the $A_{1-x}A_x'BO_{3-b}$ thin-film-based active and passive device/sensor parameters, as well as for interpretation of the experimental results in these fields, it is necessary to create new physical-mathematical concepts and modelling

methods of characterization of the above mentioned parameters with the new approaches as is pointed out in a)-e).

Acknowledgment *– This work was supported by the RA MES State Committee of Science, in the frames of the research project №* SCS *16YR-2B041.*

REFERENCES

1. Ferroelectric thin film field effect transistors based on $ZnO/BaTiO_3$ heterostructures / **M. Brandt, H. Frenzel, H. Hocmuth,** et al // J. Vac. Sci. Technol. B.- 2009. - P. 1789-1793.
2. **Scott, J. F**. Applications of Modern Ferroelectrics // *Science*.- 2007.- V.315.- P. 954–959.
3. **Gevorgian S.** Ferroelectrics in Microwave Devices, Circuits and Systems.- Springer-Verlag London Limited, 2009.- 394p.
4. **Damjanovic D., Muralt P., and Setter N.** Ferroelectric Sensors//IEEE sensors Journal.- 2001.- V.1.- P.191-206.
5. **Muralt P.** Ferroelectric thin films for microsensors and actuators: a review// J. Micromechan. Microeng. - 2000. - V.10.-P.136-146.
6. **Ling Z., Leach C., Fzeer R.** Heterojunction gas sensors for environmental NO_2 and CO_2 monitoring // J. of European Ceram. Society.- 2001.- V.21.-P.1977-1980.
7. **Poghossian A., Schöning M.J.** Silicon-Based Chemical and Biological Field-Effect Sensors // Encyclopedia of Sensor. Eds. C.A. Grimes, E.C. Dickey, M.V. Pishko.- 2006.-V. 9.-P.-463-533.
8. pH-sensitive properties of barium strontium titanate (BST) thin films prepared by pulsed laser deposition technique / **V. V. Buniatyan, M. H. Abouzar, N. W. Martirosyan, et al //** Phys. Status Solidi.- 2010.- A 207, No. 4.-P.824–830.
9. Ferroelectric Materials for Microwave Tunable applications /**A.K. Tagantsev, V.O. Sherman, K.F. Astafiev, et al//** J. of Electroceramics .- 2003.- V.11.-P.11-66.
10. Dielectric model of point charge defects in insulating paraelectric perovskites / **V. Buniatyan, N. Martirosyan, A.Vorobiev, et al //** Journal of Applied Physics. -2011.- 110.- P. 094110-1-11.
11. **Sze S.M.,. Ng K.K.** Physics of semiconductor devices.-Thirdrd ed.-Wiley-Interscience. Hoboken, N.J., 2007.- 832p.
12. **Astafiev K. F., Tagantsev A. K., and Setter N.** Quasi-Debye microwave loss as an intrinsic limitation of microwave performance of tunable components based on $SrTiO_3$ and $Ba_xSr_{1-x}TiO_3$ ferroelectrics // Journal of Applied Physics.-2005.- 97. -P.014106.

Վ.Վ. ԲՈՒՆԻԱԹՅԱՆ, Վ.Կ. ԲԵԳՈՅԱՆ, Հ.Հ. ՀՈՎՆԻԿՅԱՆ, Ա.Ա. ԴԱՎԹՅԱՆ

ՆՈՒՐԲ ԹԱՂԱՆԹԱՅԻՆ ՄԵՏԱՂ - $Ba_xSr_{1-x}TiO_3$- ՄԵՏԱՂ ԿԱՌՈՒՑՎԱԾՔՆԵՐԻ C-V, G-V ԲՆՈՒԹԱԳՐԵՐԸ

Առաջարկվել է նուրբ թաղանթային մետաղ-$Ba_xSr_{1-x}TiO_3$- մետաղ կառուցվածքների C-V, G-V կախվածությունների բնութագրման նոր մոդել: Ստացվել են C-V, G-V և կորուստների անկյան տանգենսի կախվածությունների անալիտիկական արտահայտություններ: Տեսական արդյունքները համեմատվել են փորձնական տվյալների հետ՝ ստանալով լավ համապատասխանություն:

Առանցքային բառեր. ֆերոէլեկտրիկական, թթվածնային վականսիա, *C-V* կախվածություն, Պուլ-Ֆրենկել էմիսիա.

В.В. БУНИАТЯН, В.К. БЕГОЯН, Г.А. ОВНИКЯН, А.А. ДАВТЯН

C-V, G-V ХАРАКТЕРИСТИКИ МЕТАЛЛ- $Ba_xSr_{1-x}TiO_3$- МЕТАЛЛ ТОНКОПЛЕНОЧНЫХ СТРУКТУР

Предложена новая модель для *C-V* (*g-V)* характеристик металл- $Ba_xSr_{1-x}TiO_3$- металл тонкопленочных структур. Получены аналитические выражения для C-V, g-V и тангенса угла потерь. Сравнение теоретических результатов с экспериментальными показало хорошее совпадение.

Ключевые слова*:* ферроэлектрик, кислородная вакансия, C-V зависимость, эмиссия Пуля-Френкеля.

УДК 536.5 (35)

П.А. ШИРИНЯН, Г.Г. КИРАКОСЯН, В.С. МЕЛКОНЯН

УПРАВЛЕНИЕ ЦИФРОВЫМ ПОТЕНЦИОМЕТРОМ НА ОСНОВЕ ПЛАТФОРМЫ ARDUINO С ПОМОЩЬЮ ПРОГРАММНОГО ПАКЕТА MATLAB

Рассматриваются основные области применения и схемы включения цифровых потенциометров (ЦП). Приводится методика разработки программного управления интегральным ЦП MCP42010 на основе платформы ARDUINO с помощью программного пакета MATLAB.Реализован действующий макет системы управления ЦП MCP42010 в режиме переменного (управляемого) сопротивления.

Ключевые слова: цифровой потенциометр, переменное сопротивление, настройка, ARDUINO, MATLAB.

Введение. Практически каждая электронная схема содержит элементы, предназначенные для заводской подстройки характеристик или оперативного